Nonlinear dynamic load-displacement response of foundation piles under progressive damage

Prendergast, Luke; Gavin, Kenneth

Publication date
2018

Document Version
Final published version

Published in
Proceedings of 7th Transport Research Arena TRA 2018

Citation (APA)
Prendergast, L., & Gavin, K. (2018). Nonlinear dynamic load-displacement response of foundation piles under progressive damage. In *Proceedings of 7th Transport Research Arena TRA 2018: Vienna, Austria*

Important note
To cite this publication, please use the final published version (if applicable).
Please check the document version above.

VIENNA 2018 TRA
TRANSPORT RESEARCH ARENA
A digital era for transport
solutions for society, economy and environment

Proceedings of 7th Transport Research Arena TRA 2018, April 16-19, 2018, Vienna, Austria

Nonlinear dynamic load-displacement response of foundation piles under progressive damage

Luke J. Prendergast a,*, Kenneth Gavin a

[a]*Faculty of Civil Engineering and Geosciences, Delft University of Technology, Building 23, Stevinweg 1 / PO-box 5048, 2628 CN Delft / The Netherlands*

Abstract

Soil supporting foundations for infrastructural assets such as bridges are repeatedly subjected to dynamic loading from passing traffic. The load-displacement characteristics are nonlinear at even small to medium strains, however this effect is mostly modelled using secant stiffness models with effective linear stiffness. This simplification enables a pseudo linear model to encapsulate the effects of a nonlinear system with some accuracy. Linear models have a frequency related to the amplitude of the load used to specify the secant stiffness. Nonlinear models, however, have a range of frequencies due to the changing stiffness of the system resulting from the amplitude of the input load. There is growing uncertainty surrounding the response of foundation systems to damage effects. In particular scour erosion, which is the term used to describe removal of soil from around foundation elements by hydraulic action, presents a significant hazard to infrastructure and is becoming more prevalent with increased flooding risk due to climate change effects. This paper describes a numerical framework to incorporate a basis for nonlinearities in the load-displacement response modelling of pile foundations. The Newmark-Beta nonlinear integration solver is implemented in the study. A case study is presented of a pile foundation subjected to a range of load types and progressive scour damage, and the calculated response from the various conditions is evaluated. Periodic loads of varying amplitude are implemented. Effective linear models are developed based on the secant stiffness approach and compared to the nonlinear systems. The paper presents the numerical basis for the analysis, results of the case study and advice on modelling issues relevant to analyses of this nature.

Keywords: Foundation, Damage, Piles, Nonlinear, Load-Displacement

* Corresponding author. Tel.: +31 (0)15 27 88735
E-mail address: l.j.prendergast@tudelft.nl

Nomenclature

A	API factor accounting for static or cyclic loading
A	Cross-sectional area (m^2)
C	Damping matrix
E	Young's modulus (kN/m^2)
F	External force (N)
$\mathbf{F_s}$	Restoring force (N)
I	Moment of inertia (m^4)
K	Stiffness matrix
k	Coefficient of subgrade reaction (kN/m^3)
L	Finite-Element length (m)
M	Mass matrix
p_u	Ultimate lateral resistance (kN/m)
p	Soil reaction (kN/m)
ρ	Density (kg/m^3)
t	Time (s)
x	Depth into ground (m)
$\{\mathbf{x}\}$	Dynamic displacement (m)
$\{\dot{\mathbf{x}}\}$	Dynamic velocity (m/s)
$\{\ddot{\mathbf{x}}\}$	Dynamic acceleration (m/s^2)
y	Lateral soil displacement (m)

1. Introduction

Infrastructure Maintenance Management (IMM) is concerned with the preservation and protection of infrastructural assets such as bridges or earth structures against natural deterioration and damage. Worldwide, many assets are approaching or have exceeded their original design lives so a concerted effort to extend the useable life of these systems is being made (Reale et al. 2016; Reale et al. 2017). During recent times, in many parts of the world, traffic volumes have increased as has the traffic load (Leahy et al. 2016). Moreover, climate change is having a deleterious effect on asset performance, with weather related loading becoming problematic (Martinović et al. 2016; Prendergast et al. 2016a). These trends are putting an increased stress on an already aging network, and has given rise to the field of Structural Health Monitoring (SHM) (Farrar & Worden 2007). Traditionally, SHM comprised solely of the visual inspection of assets, and the recording of generally subjective condition ratings. Overtime, this subjectivity has posed problems, in that a given analyst may mark a defect as not critical, when it may be of significance to the continued safe operation of the asset. Secondly, due to budget and man-power constraints, these types of inspections were generally carried out at discrete intervals, even as long as one year apart. Due to the increased climate-induced and man-made stresses on assets, annual inspections are no longer adequate. The field of SHM has developed and grown significantly in recent years with the increased availability of sensors and instruments that can remotely monitor assets for specific damage over time. This paper is concerned with foundation damage, in particular the erosion of foundation soil from around piles. Section 1.1 presents a brief introduction to this process and section 1.2 presents a brief overview of existing instruments and methods used to monitor foundations against this damage.

1.1. Foundation damage

The type of damage under discussion in this paper is scour erosion, the removal of material from around foundation elements by adverse hydraulic action (Hamill 1999; Prendergast et al. 2017). Scour erosion occurs due to the presence of obstacles, such as a foundation, obstructing flow and can occur under relatively benign flow conditions. During flooding, scour can occur rapidly with ramifications for foundation capacity and the potential for significant settlements.

1.2. SHM approaches for foundation damage

Many authors have developed methods/instruments capable of indirect or direct scour measurement, in a SHM framework. Direct scour measurement includes sensors such as Float-Out Devices and Tethered Buried Switches (Briaud et al. 2011; Hunt 2009), which float out of the soil when scour reaches their installed depth. This causes

the sensor to change orientation, thus triggering a signal. A different type of sensor based on Time-Domain Reflectometry (TDR) uses changes in dielectric permittivity between materials to monitor the location of the soil-water interface relative to a fixed probe (Yu 2009; Fisher et al. 2013). Similarly, Ground Penetrating Radar (GPR) systems can be used to detect and monitor scour holes using high frequency electromagnetic waves, which are partially reflected as they pass through different media (Forde et al. 1999; Anderson et al. 2007). GPR is readily suited to discrete scour assessments, but not so adept at continuous permanent monitoring. Sound wave devices such as Sonic Fathometers (Nassif et al. 2002; Prendergast & Gavin 2014; Fisher et al. 2013), Reflection Seismic Profilers (Anderson et al. 2007; Prendergast & Gavin 2014) and Echo Sounders (Anderson et al. 2007) are systems that emit sonic pulses which can locate the soil-water interface, and hence the scour depth. These systems use a similar approach to the radar-based methods. There have been a variety of systems developed that rely on the installation of rods into the soil near a foundation. For example, Magnetic Sliding Collars (MSC) (Hunt 2009; Prendergast & Gavin 2014) are a type of system which involves monitoring the movement of a gravity-controlled sensor sitting on the streambed surrounding a driven rod. The sensor falls with increasing scour depth relative to the rod and this motion causes magnetic switches located along the rod to close, which break a circuit and thus indicates the depth of the sensor. Another such system is the Wallingford 'Tell-Tail' Device (De Falco & Mele 2002), which consists of motion sensors tethered to a rod that detect bed movements as sediments are scoured to their level. Zarafshan et al. (2012) describe the development of a system which uses changes in the vibration frequency of a driven rod to detect scour, as is measured using a Fibre-Bragg Grating (FBG) sensor. Fig. 1(b) shows a schematic of some of these instruments.

In tandem with the development of systems and sensors capable of direct scour measurement, other analysis procedures have been developed to indirectly measure scour using the dynamic response of a bridge structure. Scour is effectively a change in the boundary condition of the structure, and this change manifests itself as a change in the dynamic properties (Doebling et al. 1996; Prendergast et al. 2018). Many authors have investigated the effect of scour on the dynamic properties of bridges with a view to using these measurements to detect and monitor scour (Foti & Sabia 2011; Briaud et al. 2011; Klinga & Alipour 2015; Prendergast et al. 2016a; Prendergast et al. 2016b; Prendergast et al. 2017; Bao et al. 2017; Chen et al. 2014).

In this paper, scour is considered as the lowering of the soil level relative to a foundation pile, increasing the cantilevered length and reducing the soil contact area. The resulting effect on the nonlinear dynamic displacements of a pile under external loading will be assessed in this paper.

2. Nonlinear dynamical behaviour and modelling

Nonlinear behaviour is characterised primarily by non-conformance to the principle of superposition. In linear systems, a doubling of a forcing function leads to a doubling of the displacement response (generally speaking). In nonlinear theory, this is not necessary the case. There are three basic classifications for nonlinearity (Tedesco et al. 1999): (i) Material Nonlinearity, (ii) Large Displacements (Rotations) and Small-Strains, (iii) Large Displacements (Rotations) and Large-Strains. This paper deals with case (i), material nonlinearity of the soil stress-strain response (the load-displacement, *p-y* response is actually considered – an analogue to stress-strain). Section 2.1 describes the nonlinear soil model adopted in the present study, namely the American Petroleum Institute (API) model (API 2007). To solve this system, an unconditionally stable implicit integration scheme without equilibrium iterations (for simplicity) is considered. This is described in section 2.2. Section 2.3 describes how to generate effective linear secant models.

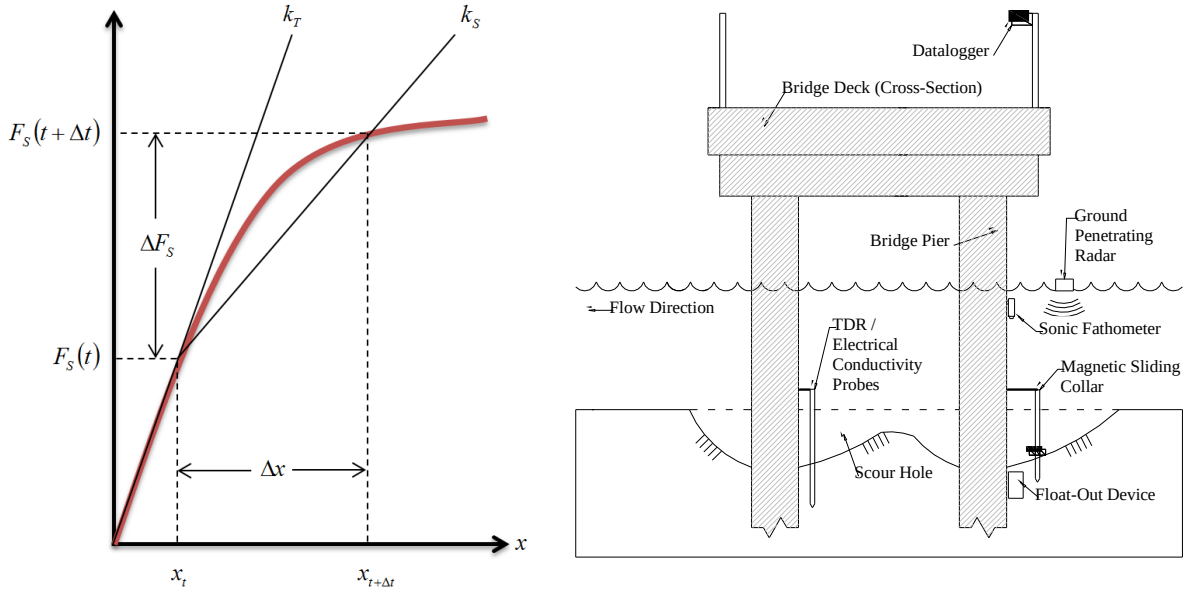

(a) (b)

Fig. 1 (a) Nonlinear load-displacement schematic (Tedesco et al. 1999), (b) Direct scour measurement devices and instruments (Prendergast & Gavin 2014)

2.1. API soil model

The lateral (horizontal) soil response is characterised by a set of soil reaction – lateral displacement (*p*-*y*) curves. The hyperbolic *p*-*y* formulation for sand as specified in the API design code (API 2007) is shown in Eq. (1).

$$p = Ap_u \tanh\left(\frac{kx}{Ap_u} y\right) \quad [1]$$

where p_u is the ultimate resistance at depth 'x' below the ground surface (kN/m), k is the constant coefficient of subgrade reaction (kN/m^3), A is an empirical factor accounting for static or cyclic external loading, y is the lateral deflection (m). Numeric values for k are specified in the API design code (API 2007). k depends on the soil density (or friction angle) and varies for saturated and unsaturated conditions. Eq. (1) describes the nonlinear soil load-displacement response over a relatively large range. In an iterative updating scheme for nonlinear modelling, the tangent stiffness (**d**p/**d**y) is required, obtained by differentiating p with respect to y as shown in Eq. (2).

$$\frac{\mathbf{d}p}{\mathbf{d}y} = Ap_u \frac{\frac{kx}{Ap_u}}{\cosh^2\left(\frac{kxy}{Ap_u}\right)} \quad [2]$$

2.2. Newmark-Beta method

The Newmark-Beta method modified to solve nonlinear dynamic systems with material nonlinearity is described herein. Nonlinear soil stiffness (load-displacement) response is characterized by Eq. (1) shown above (see Fig. 1(a)). The tangent stiffness used in the incremental equations herein, is derived from Eq. (2).

For models with material nonlinearity, the incremental equation of motion for a multi-degree-of-freedom (MDOF) system may be formulated as in Eq. (3)

$$[\mathbf{M}]\Delta\{\ddot{\mathbf{x}}\} + [\mathbf{C}]\Delta\{\dot{\mathbf{x}}\} + \mathbf{F_S}(t+\Delta t) - \mathbf{F_S}(t) = \Delta\{\mathbf{F}\} \quad [3]$$

Where **[M]** is the mass matrix, **[C]** is the damping matrix, $\mathbf{F_s}$ is the restoring force matrix and **F** is the external forcing function.

The acceleration at time $t+\Delta t$ is given by Eq. (4).

$$\{\ddot{\mathbf{x}}\}_{t+\Delta t} = \frac{4}{(\Delta t)^2}\left(\{\mathbf{x}\}_{t+\Delta t} - \{\mathbf{x}\}_t - \Delta t\{\dot{\mathbf{x}}\}_t\right) - \{\ddot{\mathbf{x}}\}_t \quad [4]$$

To express Eq. (4) incrementally, assume $\{\mathbf{x}\}_{t+\Delta t} = \{\mathbf{x}\}_t + \Delta\{\mathbf{x}\}$ and $\{\ddot{\mathbf{x}}\}_{t+\Delta t} = \{\ddot{\mathbf{x}}\}_t + \Delta\{\ddot{\mathbf{x}}\}$. Eq. (4) can be re-written as Eq. (5).

$$\Delta\{\ddot{\mathbf{x}}\} = \frac{4}{(\Delta t)^2}\left[\Delta\{\mathbf{x}\} - \Delta t\{\dot{\mathbf{x}}\}_t - \frac{(\Delta t)^2}{2}\{\ddot{\mathbf{x}}\}_t\right] \quad [5]$$

Similarly, the velocity at time $t+\Delta t$ is given by Eq. (6).

$$\{\dot{\mathbf{x}}\}_{t+\Delta t} = \{\dot{\mathbf{x}}\}_t + \frac{\Delta t}{2}\left(\{\ddot{\mathbf{x}}\}_t + \{\ddot{\mathbf{x}}\}_{t+\Delta t}\right) \quad [6]$$

To obtain Eq. (6) in incremental form, substitute $\{\dot{\mathbf{x}}\}_{t+\Delta t} = \{\dot{\mathbf{x}}\}_t + \Delta\{\dot{\mathbf{x}}\}$ and $\Delta\{\dot{\mathbf{x}}\}$ can be expressed in Eq. (7).

$$\Delta\{\dot{\mathbf{x}}\} = \frac{2\Delta\{\mathbf{x}\}}{\Delta t} - 2\{\dot{\mathbf{x}}\}_t \quad [7]$$

Substituting Eq. (5) and Eq. (7) into Eq. (3), and some arranging, yields Eq. (8).

$$[\mathbf{M}]\left(\frac{4\{\dot{\mathbf{x}}\}_t}{\Delta t} + 2\{\ddot{\mathbf{x}}\}_t\right) + 2[\mathbf{C}]\{\dot{\mathbf{x}}\}_t + \left(\frac{4[\mathbf{M}]}{(\Delta t)^2} + \frac{2[\mathbf{C}]}{\Delta t} + [\mathbf{K}]_T\right)\Delta\{\mathbf{x}\} = \Delta\{\mathbf{F}\} \quad [8]$$

Eq. (8) can be written as Eq. (9).

$$[\hat{\mathbf{K}}]_T \Delta\{\mathbf{x}\} = \Delta\{\hat{\mathbf{F}}\} \quad [9]$$

Where $[\hat{\mathbf{K}}]_T$ and $\Delta\{\hat{\mathbf{F}}\}$ are the effective tangent stiffness and effective incremental force matrices respectively. $[\hat{\mathbf{K}}]_T$ is given by Eq. (10) and $\Delta\{\hat{\mathbf{F}}\}$ by Eq. (11).

$$[\hat{\mathbf{K}}]_T = \frac{4[\mathbf{M}]}{(\Delta t)^2} + \frac{2[\mathbf{C}]}{\Delta t} + [\mathbf{K}]_T \quad [10]$$

$$\Delta\{\hat{\mathbf{F}}\} = \Delta\{\mathbf{F}\} + [\mathbf{M}]\left(\frac{4\{\dot{\mathbf{x}}\}_t}{\Delta t} + 2\{\ddot{\mathbf{x}}\}_t\right) + 2[\mathbf{C}]\{\dot{\mathbf{x}}\}_t \quad [11]$$

Incremental displacement can be calculated from Eq. (9). The incremental velocity and acceleration can thus be obtained by substituting the incremental displacement into Eq. (7) and Eq. (5) respectively. By adding the incremental acceleration, velocity and displacement to the values at time *t*, enables calculation of the kinematics at $t+\Delta t$.

2.3. Effective linear secant stiffness models

Effective linear models utilizing the secant stiffness at a specifiable operational strain are created in this paper to compare to the full nonlinear responses. A secant stiffness is specified as an acting strain level for each spring (displacement normalized by pile diameter), and the actual corresponding displacements (*y* in Eq. (1)) are calculated. The linear stiffness is then obtained as *p*/*y* at *y* specified, see Eq. (1).

3. Analysis

Table 1 outlines the geometrical and material properties of the model developed in this paper. Fig. 2 shows the API *p-y* curves that are implemented in the present analysis. Fig. 3 shows a schematic of the model used.

Table 1. Model properties

Property	Value	Unit
Diameter	0.3	m
Thickness	0.01	m
Length	10	m
Un-scoured embedment	5	m
Pile Young's modulus	$2x10^{11}$	N/m^2
Soil effective unit weight	10	kN/m^3

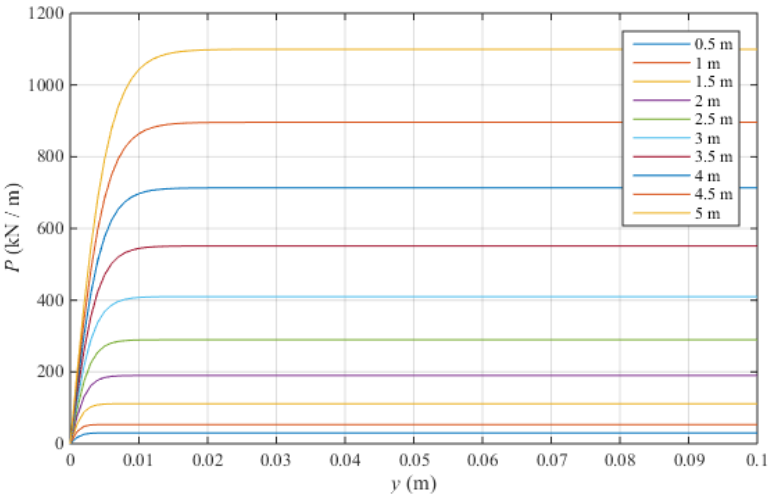

Fig. 2 p-y curves used in present study

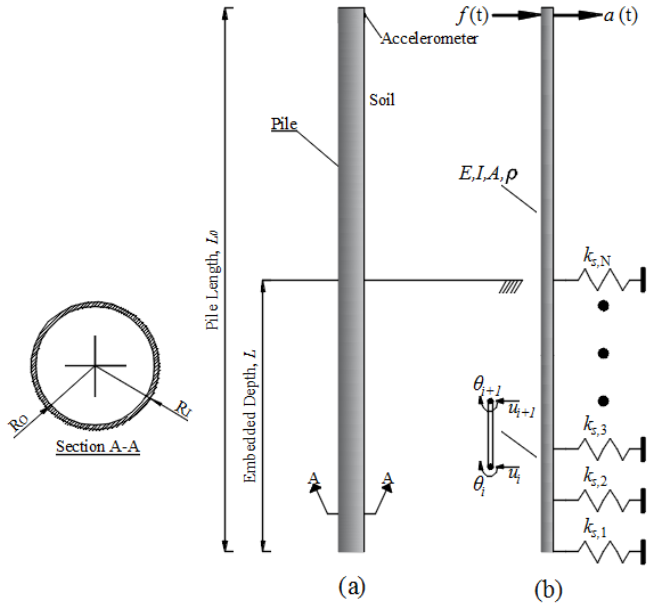

Fig. 3 Pile schematic for example pile (a) Physical schematic of system, (b) Numerical schematic

3.1. Components of response

To highlight the difference in signals under different types of soil impedance characteristic, (i) initial stiffness only, and (ii) fully nonlinear *p-y*, an analysis is carried out whereby a load is applied incrementally to the pile head then released. The results are shown in Fig. 4. A load is incrementally applied for 5 seconds up to a peak value of 5 kN, and is subsequently released, see Fig. 4(a). The resulting pile head displacement under linear (initial) stiffness and nonlinear stiffness is shown in Fig. 4(b). The linear response is shown in red and the nonlinear response is shown in blue. For clarity, only 1s worth of signal is shown, immediately after release of the applied load. Fig. 4(c) shows the results of applying a Fourier transform to the signals. A Fourier transform is applied to the full length of the generated signals (20 seconds). The nonlinearity is very evident in this plot. The linear model has a frequency at approximately 6.7 Hz. The nonlinear signal has a range of frequencies present between 6 Hz and 6.7 Hz.

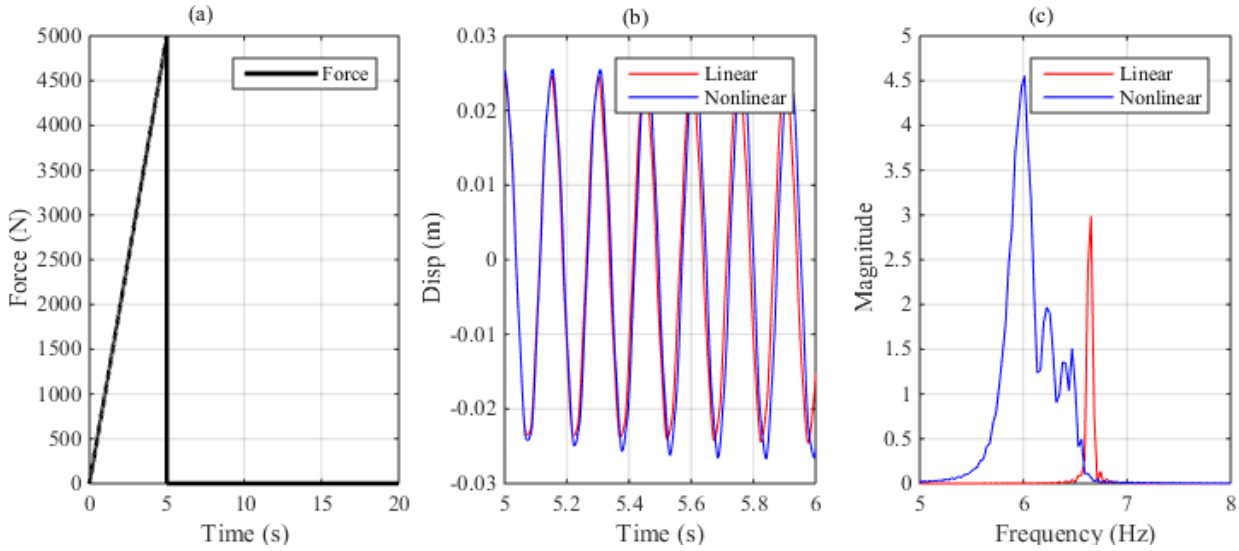

Fig. 4 Linear and nonlinear analysis (a) Load applied, (b) displacements for linear and nonlinear, (c) Frequency content

3.2. Periodic load

To simulate external loading applied to the pile head due to environmental or other loading sources, periodic loads are applied to the models herein to highlight the variations in the response signals for the different stiffness models implemented. Two periodic loads of f=0.1 Hz with maximum amplitudes of 1 kN and 10 kN respectively are applied for 8 seconds, then released to allow the models freely vibrate. The results for 1 second worth of vibration after release of the load are shown in Fig. 5. Fig. 5(a) shows the result for the initial stiffness model only. As is evident, the frequency for both the 1 kN and 10 kN loads are the same, as the stiffness is unchanged with the increased load amplitude. Fig. 5(b) shows the result when a secant stiffness corresponding to a strain of 5% is applied to each soil spring. As evident, the overall frequency of both signals (1 kN and 10 kN) is lower than in the case (a), since a lower operational stiffness is at play. However, the frequency of both the 1 kN and 10 kN signals are the same, as there is no amplitude-dependent stiffness. Finally, Fig. 5(c) shows the result for the fully nonlinear model. For this case, the 1 kN and 10 kN signals have different amplitudes *and* frequency content (denoted by the gradual misalignment of the peaks over the duration of the signal).

3.3. Foundation damage

In this section, the results of applying 1m of scour 'damage' to each model is investigated. 1m of scour is modelled as the removal of two springs from the top of the pile (springs are spaced at 0.5m). The initial linear and full nonlinear models are compared. The loading is similar to that applied in the previous section, i.e. a periodic load of f=0.1Hz with a maximum amplitude of 5 kN. Fig. 6(a) shows the signals generated for 0m and 1m scour for the case where the soil model remains in the linear small-strain region. Fig. 6(b) shows the frequency content of the signals in (a). Fig. 6(c) shows the results for 0m and 1m scour when the fully nonlinear model is adopted. Fig. 6(d) shows the frequency content of the signals in part (c). The nonlinear model has a wider distribution of frequencies at both scour depths (0m and 1m), with the mean frequency being lower than

the linear-only model. This is to be expected, as a range of operating stiffness (amplitude dependent) is at play in this problem. The results highlight that even moderate nonlinearity has a profound effect on the calculated frequency responses under scour damage for piles.

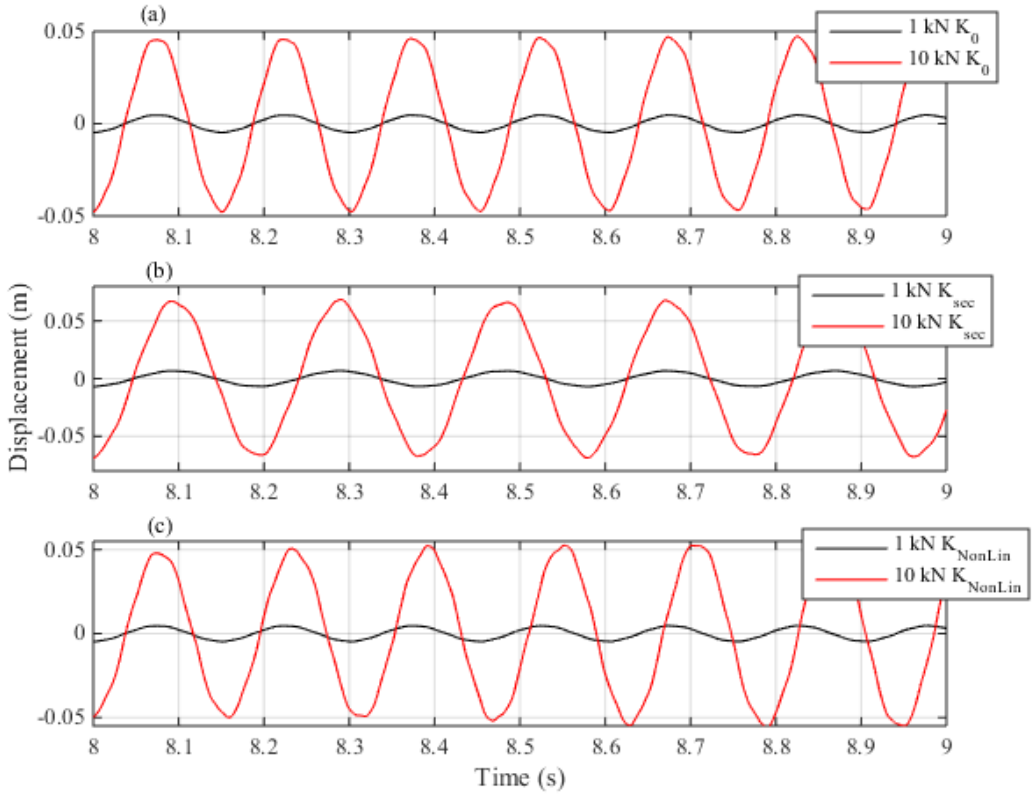

Fig. 5 Comparison of Initial Linear, Secant and Nonlinear signals under 1kN and 10kN maximum periodic load *f*=0.1Hz

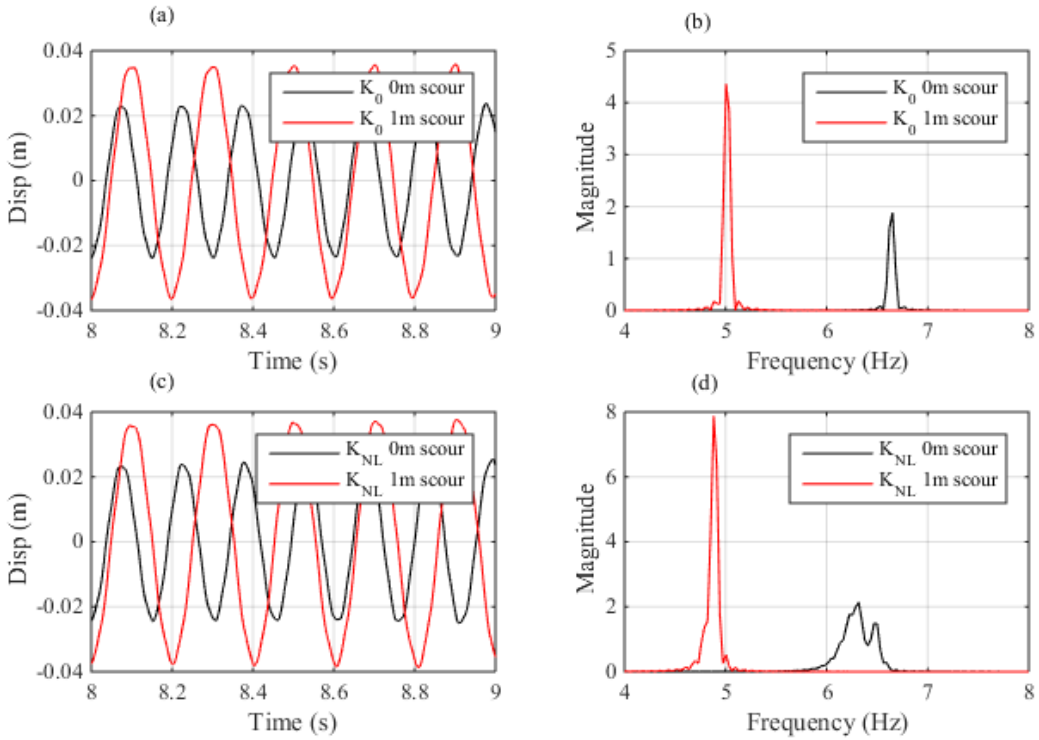

Fig. 6 Effect of scour on linear and nonlinear response spectra (a) 0m and 1m scour for linear model, (b) Frequency of signals in (a), (c) 0m and 1m scour for nonlinear model, (d) Frequency content of signals in (c)

4. Concluding remarks

In this paper, the effect of simple nonlinear dynamic soil-structure interaction on signals from a pile are studied with a view to ascertaining some insight on the potential effect on damage modelling for scour applications. A nonlinear *p-y* model based on the American Petroleum Institute method is developed and implemented in a nonlinear-elastic modelling framework, in the absence of damping. The model is used to generate response signals from a pile due to incident periodic loading in the presence of scour. The scoured signals from both the nonlinear and linear stiffness models are compared. Results show that even moderate nonlinearity introduces a wider spectrum of operating frequencies when a Fourier analysis is carried out. This wider spectrum could introduce difficulties for the accurate detection of scour in a vibration-based structural health monitoring framework.

Only the primary backbone curve model is introduced in this paper, with the assumption that unloading follows the loading path. Future work will consider inelastic recovery, cyclic hysteresis and the resulting introduction of damping to the model.

Acknowledgements

The research was partly funded by financial support from the European H2020 project SAFE-10-T (Project No. 723254) and the Department of Geoscience and Resource Engineering at TU Delft.

References

Anderson, N.L., Ismael, A.M. & Thitimakorn, T., 2007. Ground-Penetrating Radar : A Tool for Monitoring Bridge Scour. *Environmental & Engineering Geoscience*, XIII(1), pp.1–10.

API, 2007. *API RP2A-WSD*,

Bao, T. et al., 2017. Critical insights for advanced bridge scour detection using the natural frequency. *Journal of Sound and Vibration*, 386, pp.116–133. Available at: http://dx.doi.org/10.1016/j.jsv.2016.06.039.

Briaud, J.L. et al., 2011. *Realtime monitoring of bridge scour using remote monitoring technology*, Austin, TX. Available at: http://tti.tamu.edu/documents/0-6060-1.pdf.

Chen, C.-C. et al., 2014. Scour evaluation for foundation of a cable-stayed bridge based on ambient vibration measurements of superstructure. *NDT & E International*, 66, pp.16–27. Available at: http://linkinghub.elsevier.com/retrieve/pii/S0963869514000589 [Accessed February 23, 2015].

Doebling, S. et al., 1996. *Damage identification and health monitoring of structural and mechanical systems from changes in their vibration characteristics: a literature review*, Los Alamos, New Mexico. Available at: http://www.osti.gov/energycitations/product.biblio.jsp?osti_id=249299 [Accessed May 8, 2012].

De Falco, F. & Mele, R., 2002. The monitoring of bridges for scour by sonar and sedimetri. *NDT&E International*, 35, pp.117–123.

Farrar, C.R. & Worden, K., 2007. An introduction to structural health monitoring. *Philosophical transactions. Series A, Mathematical, physical, and engineering sciences*, 365(1851), pp.303–15. Available at: http://www.ncbi.nlm.nih.gov/pubmed/17255041 [Accessed October 5, 2012].

Fisher, M. et al., 2013. An evaluation of scour measurement devices. *Flow Measurement and Instrumentation*, 33, pp.55–67. Available at: http://linkinghub.elsevier.com/retrieve/pii/S0955598613000666 [Accessed September 30, 2013].

Forde, M.C. et al., 1999. Radar measurement of bridge scour. *NDT&E International*, 32, pp.481–492.

Foti, S. & Sabia, D., 2011. Influence of Foundation Scour on the Dynamic Response of an Existing Bridge. *Journal Of Bridge Engineering*, 16(2), pp.295–304.

Hamill, L., 1999. *Bridge Hydraulics*, London: E.& F.N. Spon.

Hunt, B.E., 2009. *NCHRP synthesis 396: Monitoring Scour Critical Bridges - A Synthesis of Highway Practice*, Washington, DC.

Klinga, J. V. & Alipour, A., 2015. Assessment of structural integrity of bridges under extreme scour conditions. *Engineering Structures*, 82, pp.55–71. Available at: http://linkinghub.elsevier.com/retrieve/pii/S0141029614004398 [Accessed November 14, 2014].

Leahy, C., OBrien, E. & O'Connor, A., 2016. The Effect of Traffic Growth on Characteristic Bridge Load Effects. *Transportation Research Procedia*, 14, pp.3990–3999. Available at: http://dx.doi.org/10.1016/j.trpro.2016.05.496.

Martinović, K., Gavin, K. & Reale, C., 2016. Development of a landslide susceptibility assessment for a rail network. *Engineering Geology*, 215, pp.1–9.

Nassif, H., Ertekin, A.O. & Davis, J., 2002. *Evaluation of Bridge Scour Monitoring Methods*, Trenton, NJ.

Prendergast, L.J. & Gavin, K., 2014. A review of bridge scour monitoring techniques. *Journal of Rock Mechanics and Geotechnical Engineering*, 6(2), pp.138–149.

Prendergast, L.J., Gavin, K. & Hester, D., 2017. Isolating the location of scour-induced stiffness loss in bridges using local modal behaviour. *Journal of Civil Structural Health Monitoring*. Available at: http://link.springer.com/10.1007/s13349-017-0238-3.

Prendergast, L.J., Gavin, K. & Reale, C., 2016a. Sensitivity studies on scour detection using vibration-based systems. *Transportation Research Procedia*, 14C, pp.3982–3989.

Prendergast, L.J., Hester, D. & Gavin, K., 2016b. Determining the presence of scour around bridge foundations using vehicle-induced vibrations. *Journal Of Bridge Engineering*, 21(10).

Prendergast, L.J., Reale, C. & Gavin, K., 2018. Probabilistic examination of the change in eigenfrequencies of an offshore wind turbine under progressive scour incorporating soil spatial variability. *Marine Structures*, 57, pp.87–104. Available at: http://linkinghub.elsevier.com/retrieve/pii/S0951833917301417.

Reale, C., Xue, J. & Gavin, K., 2016. System reliability of slopes using multimodal optimisation. *Géotechnique*, 66(5), pp.413–423.

Reale, C., Xue, J. & Gavin, K., 2017. Using reliability theory to assess the stability and prolong the design life of existing engineered slopes. In *Risk Assessment and Management in Geotechnical Engineering: from Theory to Practice, ASCE Geotechnical Special Publication in Memory of the Late Professor Wilson H. Tang*. p. Accepted.

Tedesco, J.W., McDougal, W.G. & Allen Ross, C., 1999. *Structural Dynamics: Theory and Applications*,

Yu, X., 2009. Time Domain Reflectometry Automatic Bridge Scour Measurement System: Principles and Potentials. *Structural Health Monitoring*, 8(6), pp.463–476. Available at: http://shm.sagepub.com/cgi/doi/10.1177/1475921709340965 [Accessed September 22, 2013].

Zarafshan, A., Iranmanesh, A. & Ansari, F., 2012. Vibration-Based Method and Sensor for Monitoring of Bridge Scour. *Journal Of Bridge Engineering*, 17(6), pp.829–838.